Cyclizations of 4-Pentenyl, 5-Hexenyl, 6-Heptenyl, and 7-Octenyl Fluorinated Radicals: A Density Functional Theory Theoretical Study

Anne Milet* and Roger Arnaud

Laboratoire d'Etudes Dynamiques et Structurales de la Sélectivité (LEDSS), Theoretical Chemistry, UMR CNRS 5616, Université Joseph Fourier, 301 Avenue de la Chimie, BP 53X, F-38041 Grenoble Cedex 09, France

Anne.Milet@ujf-grenoble.fr

Received April 3, 2001

The cyclization reactions of the 4-pentenyl, 5-hexenyl, 6-heptenyl, and 7-octenyl fluorinated and ether radicals have been studied by a hybrid Hartree−Fock density functional method. The reliability of this approach has been confirmed in agreement with experimental data and post-Hartree−Fock projected Møller−Plesset second-order method. The analysis of the theoretical results shows that two factors are crucial for the determination of the regiochemistry and the reactivity of these reactions. The first factor is the ability of the starting radical to have a stable conformation in position to form the transition state, and the second one is the enthalpic effect of the reaction through the stability of the resulting cyclized radical. It should be pointed out that these factors are not linked to the polarity of the radicals due to the presence of CF_2 groups.

Introduction

The synthesis of many organic and bioorganic compounds requires the formation of *n*-membered rings. But, to obtain both a high reactivity and a high selectivity for cyclization reactions is still challenging. One efficient way to produce *n*-membered rings is the use of intramolecular radical cyclizations, especially to produce five- or six-membered rings. Moreover, the intramolecular nature of the radical cyclization preserves the stereochemistry of the reaction. Thus, 5-hexenyl radical cyclizations appear to be the utmost synthesis tool for making five-membered rings. Nevertheless, to gain in reactivity especially for the six-membered rings, several studies have been devoted to the reactivity of different kinds of substituted radicals. Among them, 4-pentenyl, 5-hexenyl, 6-heptenyl, and 7-octenyl fluorinated radical cyclizations have received special attention in the past decade, and the works of Dolbier and colleagues[1] provide large and accurate data sets on the reactivity and regiochemistry of these processes. The main results of these studies can be summarized as follows: (a) Perfluoro 4-pentenyl radical failed to cyclize (rate constant of $k < 10^4$ s^{-1}) contrary to the ether analogue $F_2C{=}CF{-}O{-}CF_2{-}CF_2$, which cyclizes in the exo mode to give the four-membered ring product. (b) 5-Hexenyl fluorinated radicals cyclize efficiently. In both cases, the 5-exo-cyclization leading to five-membered rings is the dominant process but no high regioselectivity has been observed. For instance, $H_2C{=}CH{-}(CF_2)_3{-}CF_2$ exhibits an endo selectivity equal to 25.7%. As previously in the case of the perfluoro 4-pentenyl radical, the rate constant of the 5-exo-cyclization of the ether analogue is enhanced with respect to the parent, non-oxo radical. (c) Cyclizations of partially fluorinated 6-heptenyl radicals such as $H_2C{=}CH{-}(CH_2)_3{-}CF_2{-}CF_2$ occur with extremely large rate constants ($k > 10^7$ s^{-1}) and high regioselectivity (94.5% of the exo product). (d) 7-Octenyl radicals display an utterly different behavior; these radicals are less reactive than the 5-hexenyl or 6-heptenyl ones and cyclize in an endo manner with the percentage of exo product less than 2.

The great reactivity of these fluorinated radicals toward intramolecular addition has been mainly explained by polar factors in relation to the electrophilic character of the CF_2 radical center.[1] However, in our opinion, it seems difficult to ascribe the large differences observed both in reactivity and in regiochemistry to only the polar effects. For instance, the comparison of the expected polar effects of the $H_2C{=}CH{-}(CH_2)_3{-}CF_2{-}CF_2$ and $H_2C{=}CH{-}(CH_2)_4{-}CF_2{-}CF_2$ radicals does not explain the disparity of behavior: the 6-heptenyl radical reacts in an exo manner, and the 7-octenyl radical reacts in an endo one; in addition, the 6-heptenyl radical exhibits a very much greater enhancement of its reactivity.

Indeed, several factors can affect these intramolecular radical reactions: polar effects, of course, but also enthalpic and entropic factors, anomeric effects, etc. The availability of good quality ab initio data is essential for the evaluation of these factors and the improvement of the comprehension of the mechanism of the radical additions. But, surprisingly enough, only the intermolecular addition of carbon-centered radicals to multiple bonds has received a great deal of attention.[2] For the former, it was well-established that the reactivity is

(1) (a) Dolbier, W. R., Jr. *Chem. Rev.* **1996**, *96*, 1557 and references therein. (b) Dolbier, W. R., Jr.; Rong, X. X.; Bartgerger, M. D.; Koroniak, H.; Smart, B. E.; Yang, Z.-Y. *J. Chem. Soc., Perkin Trans.* **1998**, *2*, 219. (c) Dolbier, W. R., Jr.; Rong, X. X.; Smart, B. E.; Yang, Z.-Y. *J. Org. Chem.* **1996**, *61*, 4824. (d) Dolbier, W. R., Jr.; Li, A.; Smart, B. E.; Yang, Z.-Y. *J. Org. Chem.* **1998**, *63*, 5687. (e) Li, A.; Shatrev, A. B.; Smart, B. E.; Yang, Z.-Y.; Lusztyk, J.; Ingold, K. U.; Bravo, A.; Dolbier, W. R., Jr. *J. Org. Chem.* **1999**, *64*, 5993.

(2) Theoretical study involving addition of fluoroalkyl radicals: (a) Arnaud, R. *New J. Chem.* **1989**, *13*, 543. (b) Bottoni, A. *J. Chem. Soc., Perkin Trans.* **1996**, *2*, 2041. (c) Korchowiec, J.; Uchimaru, T. *J. Phys. Chem. A* **1998**, *102*, 2439. (d) Korchowiec, J.; Uchimaru, T. *J. Phys. Chem. A* **1998**, *102*, 6682.

10.1021/jo0103470 CCC: $20.00
Published on Web 08/07/2001

governed by both enthalpic and polar factors.[3,4] These two factors seem to also play a determining role in the regiochemistry of these reactions.[5] On the other hand, to the best of our knowledge, theoretical approaches of intramolecular addition to double bonds are very scarce, and only Houk and Spellmeyer reported ab initio transition structures (UHF/STO-3G level) corresponding to the cyclization of the 5-hexenyl radical.[6] During the revision of the paper, Baker and Dolbier published a DFT study of the cyclizations of fluorinated 4-pentenyl radicals.[7]

Thus, in this work, we report an application of the density functional theory (DFT) to the intramolecular cyclizations of several fluorinated radicals including ether analogues. The hybrid Hartree−Fock/density functional theory (HF/DFT) method has been proven to successfully deal with intermolecular radical additions to double bonds,[2d,2c,8] and our choice is also dictated by this "inexpensive" computational model that can be applied to large systems.

Because of the large and accurate experimental data sets available for these reactions, one of the goals of this study is to examine the reliability of the HF/DFT method in reproducing the experimental trends of reactivity and regioselectivity of intramolecular cyclizations. And naturally, we also want to provide information on the factors determining the rate and the orientation of these intramolecular radical additions. On the other hand, this study will not be devoted to a conformational study of the manifold radicals. Because of the large number of conformers, such a subject deserves a complete study, which is out of the scope of this present paper.

The notation of the radicals studied is given in the following chart:

$F_2C{=}CF{-}(CF_2)_2{-}CF_2$	**5a**	$F_2C{=}CF{-}(CF_2)_3{-}CF_2$	**6a**
$F_2C{=}CF{-}O{-}CF_2{-}CF_2$	**5a′**	$F_2C{=}CF{-}O{-}(CF_2)_2{-}CF_2$	**6a′**
$F_2C{=}CH{-}(CF_2)_2{-}CF_2$	**5b**	$F_2C{=}CH{-}(CF_2)_3{-}CF_2$	**6b**
$F_2C{=}CH{-}O{-}CF_2{-}CF_2$	**5b′**	$H_2C{=}CH{-}(CF_2)_3{-}CF_2$	**6c**
$F_2C{=}CF{-}CF_2{-}CH_2{-}CF_2$	**5c**	$H_2C{=}CH{-}(CF_2)_4{-}CF_2$	**7c**
$F_2C{=}CF{-}O{-}CH_2{-}CF_2$	**5c′**	$H_2C{=}CH{-}(CH_2)_3\,CF_2{-}CF_2$	**7d**
$F_2C{=}CH{-}CF_2{-}CH_2{-}CF_2$	**5d**	$H_2C{=}CH{-}(CH_2)_4\,CF_2{-}CF_2$	**8d**
$F_2C{=}CH{-}O{-}CH_2{-}CF_2$	**5d′**		

We recall (Baldwin rules) that the endo cyclization corresponds to the radical attack on the terminal end of the alkene and leads to the larger membered ring radical product.

Computational Details

All the calculations are based on the unrestricted Kohn−Sham (UKS) approach to the DF theory[9] as implemented in the Gaussian 98 package.[10] On the grounds of previous experience,[5,7b−d] we have selected the so-called B3LYP hybrid functional.[11] Structural features (geometry optimizations, vibrational frequency, and intrinsic reaction coordinates (IRCs)) have been obtained using the 6-31G(d) split valence basis set.[12a] Frequencies and zero point energy (ZPE) corrections were calculated using the harmonic approximation without scaling. Indeed, the scaling factors for the method used are, respectively, 0.9989 and 1.0015 at 298 K and 1 atm for ΔH and ΔS.[12b] All the transition structures have been confirmed by frequency calculations, and the corresponding two minima have been established by tracing the IRC.

Basis set effects on relative energies have been tested by UB3LYP/6-311+G(2d,2p) single-point calculations. Additional post-HF calculations have been made with the projected second-order Møller−Plesset (PMP2) method. The electronic structure of some stationary points was analyzed by the natural bond orbital (NBO) method[13] employing the program G94NBO.[14] In addition, delocalization energies can be obtained using the Fock matrix deletion approach.[15] The ionization potentials have been calculated as the energy difference between ZPE-corrected total energies of the radical alkene cation and the neutral alkene.

In this work, we have not investigated a conformational study of starting radicals, but we will pay attention to the conformations of the reactive radicals; the former are those deduced from IRC calculations.

Results and Discussion

1. Geometries. Figures 1−4 display the optimized geometries of all the stationary points, minima, and transition states (TSs) of the determined reaction paths. IRC calculations indicate that the TSs corresponding to the exo and endo attacks are connected to the same starting conformer of the open radical, except for the cases of **6a′** and **8d**. Table 1 lists the values of R and θ parameters defined by Figure 1. Concerning the **5a** and **5a′** structures, it should be noted that our results disagree with those published by Baker and Dolbier.[7] They have considered the open conformation of these radicals, whereas we follow the IRC calculations and connect the TS structure to a near-attack conformation (NAC) as shown Figure 1.

First, let us discuss briefly the geometrical features of the transition states. They all exhibit intramolecular distances R between the two reaction centers in the range

(3) (a) Fischer, H. In *Free Radicals in Biology and Environment*; Minisci, F., Ed.; Kluwer: Dordrecht, Netherlands, 1997. (b) Zytowski, T.; Fisher, H. *J. Am. Chem. Soc.* **1996**, *118*, 437. (c) Zytowski, T.; Fisher, H. *J. Am. Chem. Soc.* **1997**, *119*, 12869. (d) Heberger, K.; Lopata, A. *J. Org. Chem.* **1998**, *63*, 8646.

(4) (a) Wong, M. W.; Pross, A.; Radom, L. *J. Am. Chem. Soc.* **1993**, *115*, 11050. (b) Wong, M. W.; Pross, A.; Radom, L. *J. Am. Chem. Soc.* **1994**, *116*, 6284. (c) Wong, M. W.; Pross, A.; Radom, L. *J. Am. Chem. Soc.* **1994**, *116*, 11938.

(5) Arnaud, R.; Vetere, V.; Barone, V. *J. Comput. Chem.* **2000**, *21*, 675.

(6) Spellmeyer, D. C.; Houk, K. N. *J. Org. Chem.* **1987**, *52*, 959.

(7) Baker, J. M.; Dolbier, W. R., Jr. *J. Org. Chem.* **2001**, *66*, 2662.

(8) (a) Barone, V. Recent Advances in Chemistry Density Functional Methods Part I. *Recent Advances in Computational Chemistry*; World Scientific: Singapore, 1995; Vol. I. p 287. (b) Barone, V.; Orlandini, L. *Chem. Phys. Lett.* **1995**, 246. (c) Jursic, B. S. *J. Chem. Soc., Perkin Trans.* **1997**, *2*, 637. (d) Arnaud, R.; Bugaud, N.; Vetere, V.; Barone, V. *J. Am. Chem. Soc.* **1998**, *120*, 5733.

(9) Parr, R. G.; Yang, W. *Density-Functional Theory of Atoms and Molecules*; Oxford University Press: New York, 1989.

(10) Frisch, M. J.; Trucks, G. W.; Schlegel, H. B.; Scuseria, G. E.; Robb, M. A.; Cheeseman, J. R.; Zakrzewski, V. G.; Montgomery, J. A., Jr.; Stratmann, R. E.; Burant, J. C.; Dapprich, S.; Millam, J. M.; Daniels, A. D.; Kudin, K. N.; Strain, M. C.; Farkas, O.; Tomasi, J.; Barone, V.; Cossi, M.; Cammi, R.; Mennucci, B.; Pomelli, C.; Adamo, C.; Clifford, S.; Ochterski, J.; Petersson, G. A.; Ayala, P. Y.; Cui, Q.; Morokuma, K.; Malick, D. K.; Rabuck, A. D.; Raghavachari, K.; Foresman, J. B.; Cioslowski, J.; Ortiz, J. V.; Stefanov, B. B.; Liu, G.; Liashenko, A.; Piskorz, P.; Komaromi, I.; Gomperts, R.; Martin, R. L.; Fox, D. J.; Keith, T.; Al-Laham, M. A.; Peng, C. Y.; Nanayakkara, A.; Gonzalez, C.; Challacombe, M.; Gill, P. M. W.; Johnson, B. G.; Chen, W.; Wong, M. W.; Andres, J. L.; Head-Gordon, M.; Replogle, E. S.; Pople, J. A. *Gaussian 98*, revision A.6; Gaussian, Inc.: Pittsburgh, PA, 1998.

(11) (a) Becke, A. D. *Phys. Rev. A* **1988**, *38*, 3098. (b) Lee, C.; Wang, W.; Parr, R. G. *Phys. Rev. B* **1988**, *37*, 785. (c) Becke, A. D. *J. Chem. Phys.* **1993**, *98*, 5648.

(12) (a) Description of basis set and explanation of standard levels of theory can be found in the following: Foresman, J. B.; Frisch, A. E. *Exploring Chemistry with Electronic Structure Methods*, 2nd ed.; Gaussian, Inc.: Pittsburgh, PA, 1996. (b) Scott, A. P.; Radom, L. *J. Phys. Chem.* **1996**, *100*, 16502.

(13) Reed, A. E.; Curtiss, L. A.; Weinhold, F. *Chem. Rev.* **1988**, *88*, 899.

(14) Glendening, E. D.; Reed, A. E.; Carpenter, J. E.; Weinhold, F. *NBO*, version 3.1; 1988.

(15) (a) Tyrell, J.; Weinstock, R. B.; Weinhold, F. *Int. J. Quantum Chem.* **1981**, *19*, 781. (b) Curtiss, L. A.; Pochatko, D. J.; Reed, A. E.; Weinhold, F. *J. Chem. Phys.* **1983**, *82*, 2679.

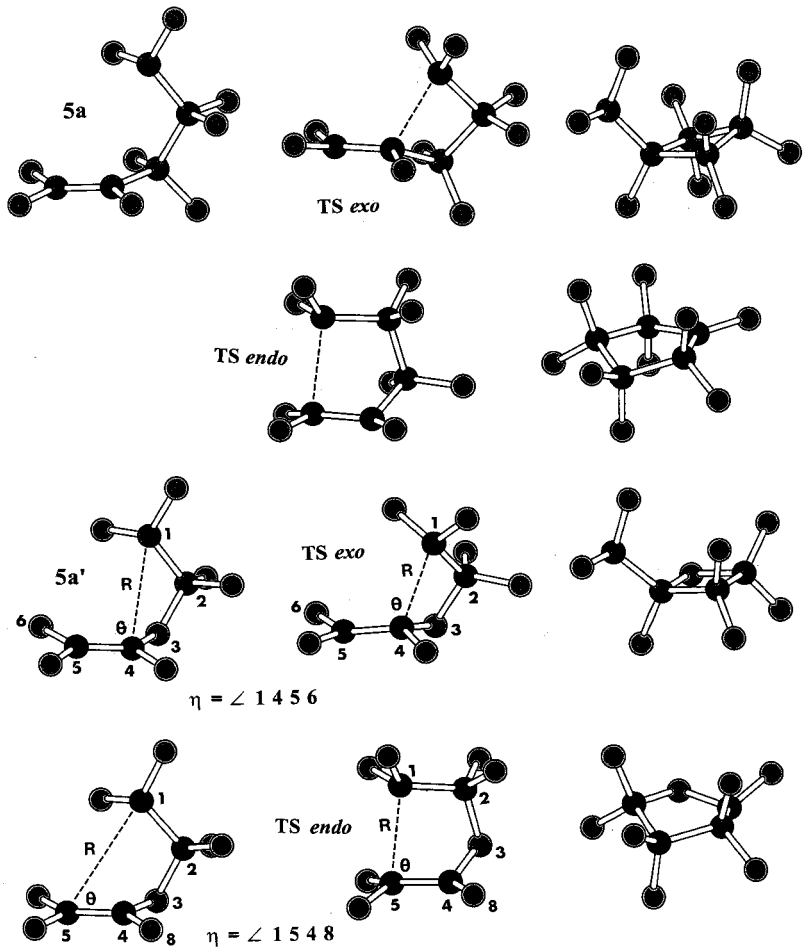

Figure 1. Optimized structures of the potential energy surface (PES) stationary points in the radical cyclization reactions of **5a** and **5a′**.

of 2.1−2.4 Å, values comparable to those obtained for intermolecular CF_3 addition to olefins.[16] In intermolecular additions, the angle (θ) of attack of the radical to the alkene lies within a narrow spectrum of values, from 105° to 112°, whatever the addition of carbon-centered radicals considered.[4,16] In contrast, in intramolecular additions, θ values in TSs present a larger range, from 84° to 120° (see Table 1). This seems to be dependent on the length of the radical arm through steric requirements: the shortest radical arm (pentenyl radical) corresponds to the largest (smallest) θ values for the exo (endo) approach.

But, the key point of this structural analysis is the comparison between the conformation of the reactive radical and the conformation of the TS. Indeed, the relative position of the reaction centers (radical center and one of the olefinic carbon atoms) in the reactive radical is crucial for the assessment of the rate constant and the orientation of the cyclizations (vide infra). Thus, we have collected in Table 1 the geometrical parameters giving the relative positions of the reaction centers in the starting radicals and in the transition stuctures.

The following conclusions can be deduced from the comparison of the data in Table 1:

(a) In the case of the cyclizations of 4-pentenyl and 5-hexenyl radicals, TSs exo and endo are both connected to starting radicals that adopt conformations favoring an exo approach (see Figures 1 and 2 and ΔR and $\Delta\theta$ values in Table 1). Indeed, according to the Bruice definition,[17] these conformations can be termed exo NACs. Because no stable endo NAC has been found, we expect that endo cyclization will be a more difficult process than exo cyclization because more energy will be required to bring the reaction centers close to each other before reaching the endo TS.

(b) When the length of the radical arm is increased to heptenyl radicals, **7c** and **7d**, the conformation issued from TSs exo and endo is between the exo and endo NACs (see Figure 3 and Table 1; in the starting radical, for both exo and endo additions, the angles of attack, θ, are lower than 90°). So, for these particular cyclizations, the conformation of the starting radical is not expected to play a determing role in the orientation of the addition. However, R values are not very large, and therefore, the starting conformers cannot be considered as "outside the NAC". Consequently, the regiochemistry of the additions of **7a** and **7b** cannot be due to a "conformational control".

(c) Finally, if the radical arm is longer (**8d**), the conformers obtained by IRC calculations are characterized by very large R distances: 5.137 Å (conformer exo) and 5.479 Å (conformer endo) (see Figure 4). These two conformers cannot be considered as NACs, and we expect,

(16) Arnaud, R. Unpublished results. UB3LYP/6-31G(d) calculations; for CF_3 addition on $F_2C{=}CXCF_3$ and $F_2C{=}CXYCF_3$ (X=H, F; Y=O, CF_2), R lies in the range of 2.260−2.380 Å.

(17) (a) Lightstone, F. C.; Bruice, T. C. *J. Am. Chem. Soc.* **1996**, *118*, 2595. (b) Bruice, T. C.; Lightstone, F. C. *Acc. Chem. Res.* **1999**, *32*, 127.

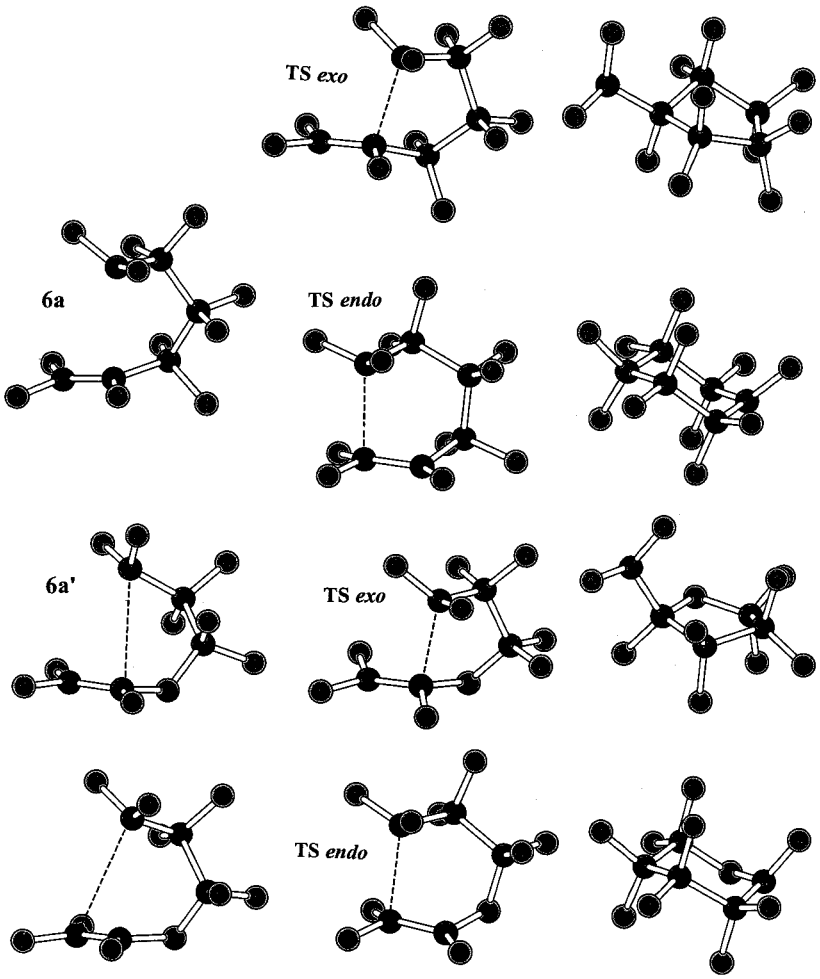

Figure 2. Optimized structures of the PES stationary points in the radical cyclization reactions of **6a** and **6a′**.

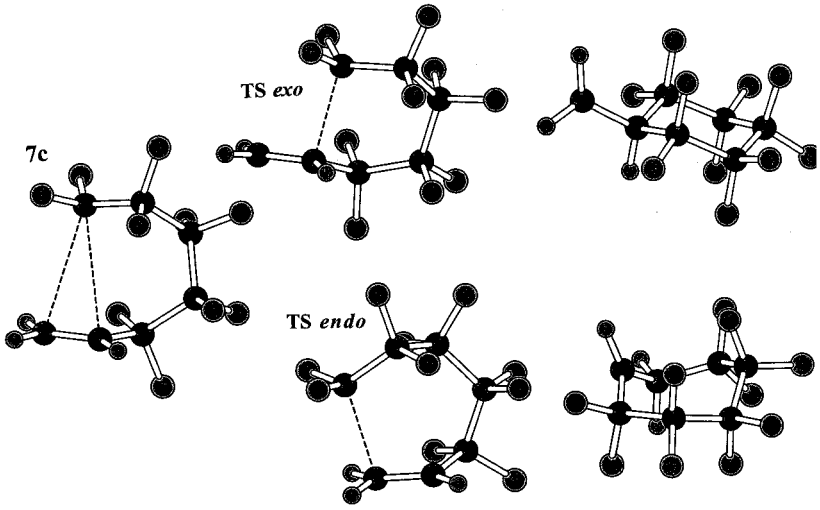

Figure 3. Optimized structures of the PES stationary points in the radical cyclization reaction of **7c**.

because of the absence of stable NACs, (a) a lower rate of cyclization of **8d** and (b) absolutely no influence of the conformation of starting radical on the regiochemistry of the intramolecular addition.

We end up this comment on geometries with a brief comparison between the structure of 4-pentenyl and 5-hexenyl radicals on one hand and that of their ether analogues on the other hand. Indeed, Beckwith[18] has suggested that the enhanced reactivity of ether analogues can be attributed to geometrical factors, the shortest C−O bond length and the lowest COC bond angle, which allow them to more easily reach the exo TSs. On the basis of *R* distances, our results support this suggestion; the *R* and ΔR values are always larger in the fluorinated radicals **5a** and **6a** exo than those in their ether analogues **5a′** and **6a′** exo (see Table 1).

(18) Beckwith, A. L. J.; Glover, S. A. *Aust. J. Chem.* **1987**, *40*, 157.

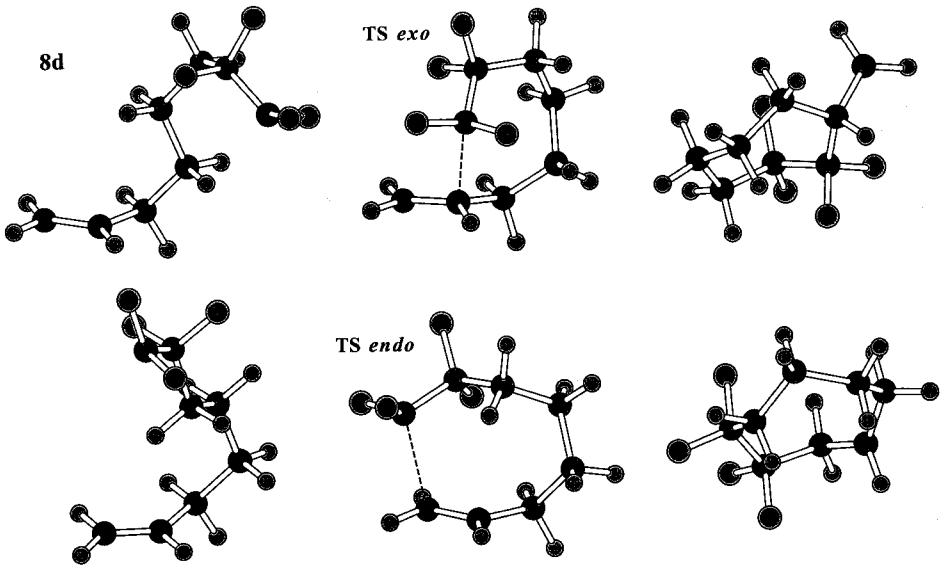

Figure 4. Optimized structures of the PES stationary points in the radical cyclization reaction of **8d**.

Table 1. Representative Geometrical Parameters Giving the Relative Position of the Reaction Centers in the Starting Radical and in the TS and the Absolute Difference between Them in Parentheses[a]

	starting radical		TS	
radicals	*R*, Å	*θ*, deg	*R*, Å	*θ*, deg
5a exo	3.048	105.9	2.123 (0.925)	118.1 (12.2)
5a endo	3.491	64.2	2.335 (1.156)	89.5 (25.3)
5a′ exo	2.854	98.6	2.167 (0.687)	114.2 (15.6)
5a′endo	3.221	58.3	2.345 (0.977)	84.0 (25.7)
6a exo	3.066	94.5	2.295 (0.771)	108.4 (3.9)
6a endo	3.268	74.1	2.334 (0.934)	94.7 (20.6)
6a′ exo	2.955	98.8	2.356 (0.600)	105.1 (6.3)
6a′ endo	3.264	77.5	2.355 (0.909)	92.4 (14.9)
7c exo	3.330	76.0	2.385 (0.945)	102.3 (26.3)
7c endo	3.274	80.8	2.400 (0.874)	103.6 (22.8)
8d exo	5.137	139.7	2.335 (2.802)	100.6 (39.1)
8d endo	5.479	78.5	2.382 (3.097)	108.8 (30.3)

[a] For the definition of geometrical parameters, see Figure 1.

2. Energies. The TS ($\Delta E^{\ddagger}$) and radical product ($\Delta_r E$) relative energies are collected in Table 2. At first glance, we can see that extension of the basis set from 6-31G(d) to 6-311+G(2d,2p) Pople basis sets has only a very limited effect on the energy barriers, $\Delta E^{\ddagger}$. This conclusion contrasts with the results obtained for bimolecular radical addition reactions.[19] This trend can probably be connected to the lower magnitude of basis set superposition error (BSSE) for unimolecular reactions. The way of treating the correlation energy, through PMP2 perturbative method or using the hydrid HF/DFT, namely, B3LYP in this study, has also a very limited effect on the $\Delta E^{\ddagger}$ values.

The situation is different for the reaction energy $\Delta_r E$, which is the energy difference between the cyclized radical and the reactive one. The exothermicity of these reactions is reduced when a large basis set is used and is enhanced using single-point PMP2 calculations. This latter trend seems to be general for all radical addition reactions, both intramolecular and intermolecular. Because the primary interest in chemical studies is often concerned with trends rather than absolute quantities, we have focused our interest on the variations in $\Delta E^{\ddagger}$ (Figure 5) and in $\Delta_r E$ (Figure 6) predicted at these various levels of calculation. Thus, despite the apparent dependence on the method used for $\Delta_r E$, it is worth noting the very good correlation for $\Delta E^{\ddagger}$ ($R = 0.991$) and $\Delta_r E$ ($R = 0.994$), which indicates that all calculations give very similar trends.

We have also added in Table 2 relative zero-point energy corrections (ΔZPE). The vibrational corrections also do not alter the ordering given by $\Delta E^{\ddagger}$ and $\Delta_r E$. Because of this good correlation, we will only have to comment on one set of results, the results obtained at the UB3LYP/6-31G(d) level. Now, let us discuss the variations of $\Delta E^{\ddagger}$ and $\Delta_r E$ in comparison with experimental data.

Table 2. Energies (Relative to the Starting Radical) (kcal mol^{-1}) for TSs and Radical Products of the Radical Cyclization Reactions; Values in Parentheses Are Relative Zero-Point Energy Corrections (ΔZPE)

	$\Delta E^{\ddagger}$			$\Delta_r E$		
radicals	B3LYP[a]	B3LYP[b]	PMP2[a]	B3LYP[a]	B3LYP[b]	PMP2[a]
5a exo	13.6 (−1.0)	13.9	14.6	−5.8 (1.6)	−4.0	−8.3
5a endo	13.7 (−0.8)	14.4	14.9	−25.4 (0.9)	−24.5	−28.2
5a′ exo	7.1 (−1.0)	7.2	8.3	−18.7 (1.7)	−16.2	−23.6
5a′ endo	11.8 (−0.9)	12.4	12.6	−29.9 (1.2)	−27.4	−34.9
5b exo	14.4 (−0.8)	14.2	15.7	−2.4 (0.7)	−1.3	−4.0
5b′ exo	9.3 (−0.8)	9.6	10.6	−11.7 (1.8)	−9.4	−15.1
5c exo	14.5 (−1.3)	15.1	15.0	−5.9 (0.3)	−3.4	−9.8
5c′ exo	9.3 (−1.2)	10.1	10.2	−15.4 (1.7)	−12.0	−20.7
5d exo	14.3 (−1.0)	14.4	15.5	−3.5 (0.5)	−1.6	−6.4
5d′ exo	11.1 (−1.1)	11.7	11.9	−9.4 (0.8)	−6.6	−13.8
6a exo	5.3 (−0.7)	5.3	5.6	−21.9 (1.0)	−19.0	−27.1
6a endo	6.1 (−0.7)	6.8	6.2	−28.4 (1.1)	−25.3	−34.0
6a′ exo	3.1 (−0.8)	2.9	3.6	−31.2 (1.2)	−28.5	−37.7
6a′ endo	6.2 (−0.7)	7.2	6.1	−32.5 (1.3)	−28.9	−39.2
6b exo	5.3 (−0.5)	5.3	6.2	−19.2 (1.4)	−17.5	−23.4
6b endo	7.5 (−0.7)	8.7	7.5	−23.0 (0.5)	−20.4	−28.4
6c exo	4.3 (−0.5)	4.2	4.2	−17.9 (0.1)	−17.1	−22.1
6c endo	5.1 (−0.3)	5.4	4.8	−28.7 (1.1)	−27.1	−33.2
7c exo	2.7 (−0.5)	2.4	2.3	−26.1 (0.3)	−24.5	−32.8
7c endo	3.3 (−0.2)	3.4	3.5	−26.7 (1.3)	−24.8	−31.9
7d exo	1.8 (−0.2)	2.5	1.7	−28.4 (0.8)	−25.7	−36.0
7d endo	2.9 (0.1)	3.9	2.7	−26.8 (1.7)	−23.6	−32.7
8d exo	7.8 (−0.1)	9.5	6.8	−20.5 (1.1)	−16.0	−28.3
8d endo	6.7 (0.1)	8.4	6.3	−25.4 (1.6)	−21.5	−30.7

[a] 6-31G(d) basis set. [b] 6-311+G(2d,2p) basis set.

(19) Arnaud, R. Unpublished results. For example, UB3LYP/6-31G(d) $\Delta E^{\ddagger}$ values for CF_3 addition on unsubstituted and substituted carbon atoms of $CH_2{=}CF_2$ are 1.3 and 3.7 kcal mol^{-1}, respectively; the corresponding $\Delta E^{\ddagger}$ values calculated at the UB3LYP/6-311+G(2d,2p)//UB3LYP/6-31G(d) level are 2.5 and 6.1 kcal mol^{-1}.

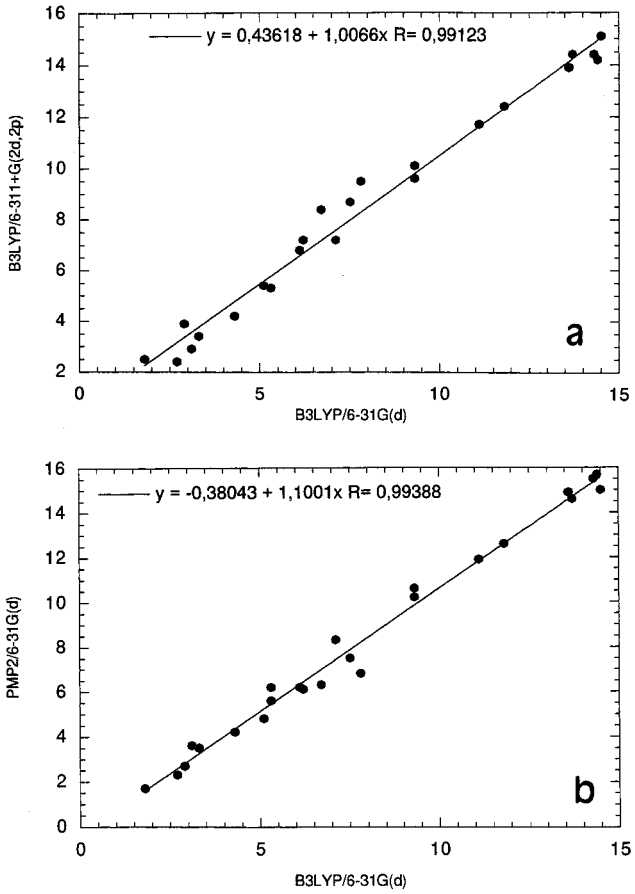

Figure 5. Correlation between energy barrier $\Delta E^{\ddagger}$ for the radical cyclization reactions calculated (a) at the UB3LYP/6-311+G(2d,2p) and UB3LYP/6-31G(d) levels and (b) at the PMP2/6-31G(d) and UB3LYP/6-31G(d) levels.

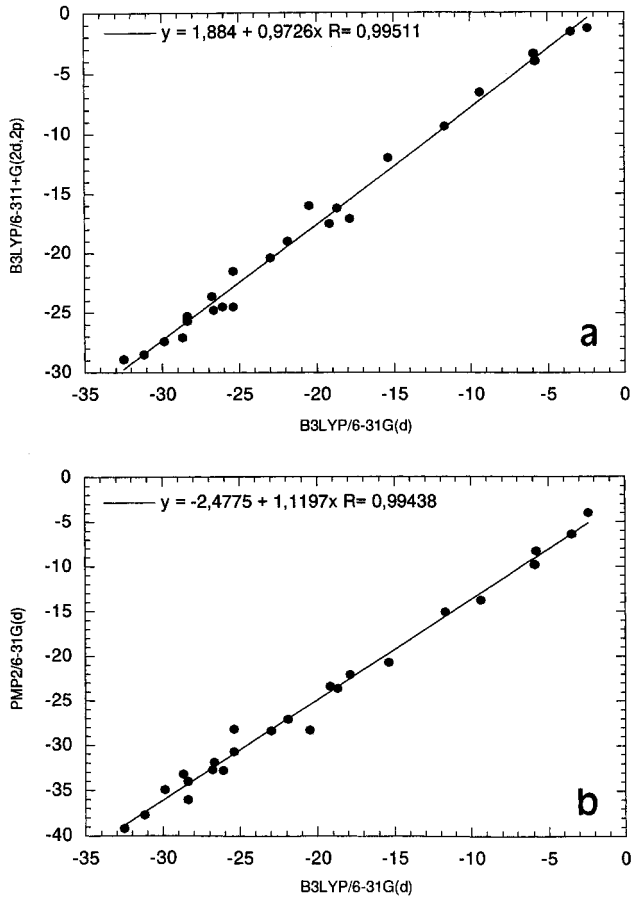

Figure 6. Correlation between reaction energy $\Delta_r E$ for the radical cyclization reactions calculated (a) at the UB3LYP/6-311+G(2d,2p) and UB3LYP/6-31G(d) levels and (b) at the PMP2/6-31G(d) and UB3LYP/6-31G(d) levels.

2.1. 4-Pentenyl Radicals. From our calculations, it follows that the barrier height corresponding to the exo cyclization of fully fluorinated radical **5a** is notably higher than the one corresponding to the cyclization of the ether analog **5a′** (13.6 vs 7.1 kcal mol^{-1}). This result is in good agreement with experimental data: the rate constant for the cyclization of **5a** is less than 10^4 s^{-1}, while **5a′** cyclizes quite efficiently with a rate constant equal to 3.8×10^5 s^{-1}.[1a] The lower exo barrier corresponds to the more exothermic process (−18.7 (**5a′**) vs −5.8 (**5a**) kcal mol^{-1}). This trend cannot be extended to the endo attack, which is predicted to be less favorable than the exo one despite the largest stability of five-membered ring adducts. The $\Delta E^{\ddagger}$(endo) − $\Delta E^{\ddagger}$(exo) difference is important in the case of **5a′**, but it is considerably reduced in the case of **5a**. It is noteworthy that this weak difference in $\Delta E^{\ddagger}$ is associated with the largest difference in $\Delta_r E$; the endo cyclized radical is more stable by about 20 kcal mol^{-1} than the exo one. This result clearly shows the influence of the heat of reaction upon relative barrier height.

As mentioned in the preceding paragraph, the greater reactivity of the ether analogue in radical cyclization was attributed to a more favorable arrangement of reaction centers in this radical. This preferential conformation of **5a′** could be attributed to oxygen lone pairs antibonding adjacent orbitals, i.e., $n_O-\sigma^*_{C_{2(4)}-X}$ delocalizations (X = H, F; see Figure 1 for the numeration). This delocalization is stronger when X = F and leads to a shortening of the $C_{2(4)}$−O bonds. Additionally, this hypothesis is supported by the increase of $\Delta E^{\ddagger}$ when fluorine atoms are progressively substituted by hydrogen atoms (**5b′**, **5c′**, and **5d′**). However, the progressive substitution of fluorine atoms by H atoms does not induce noticeable changes in the relative position of radical center and C_4 atom (see Table 1). To better appraise the eventual contribution of $n_O-\sigma^*_{C_{2(4)}-X}$ interactions to the enhancement of the reactivity of ether analogues, we have computed the $n_O-\sigma^*_{C_2-X}$ and $n_O-\sigma^*_{C_4-X}$ delocalization energies along the reaction path for the exo cyclizations of **5a′**−**5d′**. Figure 7 shows the results obtained for the cyclization of **5a′**, which are representative of the whole results.

The variations of the interaction energies are of weak amplitude. Thus, the results indicate that $n_O-\sigma^*_{C-X}$ delocalization interaction does not play a significant role in the reactivity of **5a′** and of the ether analogues.

2.2. 5-Hexenyl Radicals. In agreement with the experiments, calculations predict that these radicals cyclize more easily than the 4-pentenyl ones. For instance, the lowering of $\Delta E^{\ddagger}$ ranges from 8.3 kcal mol^{-1} for the fully fluorinated radical **6a** to 4.0 kcal mol^{-1} for the ether analogue **6a′**. In addition, cyclizations of 5-hexenyl radicals are more exothermic processes. In this set of radicals, the calculations also reproduce accurately experimental trends: (a) TS corresponding to the exo addition of **6a** lies 5.3 kcal mol^{-1} above the starting radical; this value is not high enough to prevent the exo cyclization observed experimentally. (b) A low energy

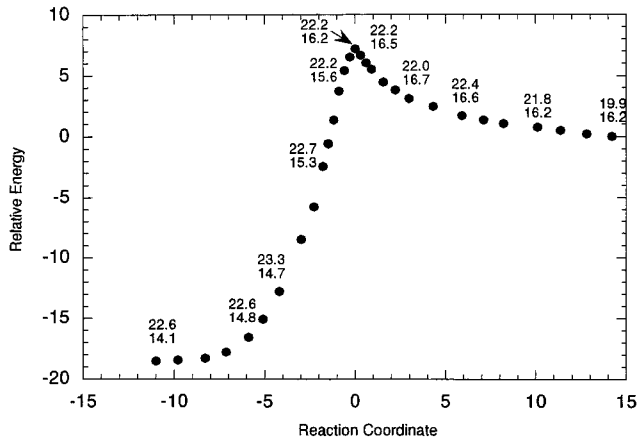

Figure 7. Potential energy as a function of the intrinsic reaction coordinate for the exo cyclization of **5a′**. The upper values are $-n_O-\sigma^*_{C_4-F}$ delocalization energies; the lower values are $-n_O-\sigma^*_{C_2-F}$ delocalization energies.

barrier equal to 3.1 kcal mol^{-1} is obtained for the cyclization of the ether analogue **6a′** in accordance with its enhanced reactivity (k_{exo}(**6a**) = 4.9 × 10^5 s^{-1}, k_{exo}(**6a′**) = 3.5 × 10^6 s^{-1}). (c) Dolbier et al.[1] pointed out that the degree of fluorination of the double bond has relatively little impact upon the rate and regiochemistry of 5-hexenyl radical cyclization, because the largest difference has been measured between radicals **6a** and **6c** (**6c** is 24 times more reactive than **6a** for the exo addition).[1a,1b] Our results support this trend; the exo additions for **6a** and **6b** occur with almost the same barrier height whereas the energy barrier is notably reduced for the cyclization of **6c**. (d) The observed regiochemistry of these additions is also well-reproduced by calculations. In both cases, the exo orientation is favored; **6c** gives the lowest regioselective cyclization (experimentally, Dolbier obtains 25% of endo product[1a]). The examination of Table 2 shows that, among the 5-hexenyl radicals investigated in this work, the lower $\Delta E^{\ddagger}$ value for the endo cyclization is obtained for **6c**.

2.3. 6-Heptenyl Radicals. On the basis of $\Delta E^{\ddagger}$ values, our results predict the following: (a) **7c** cyclizes more rapidly than **6c**. Although **7c** has not been experimentally studied, our result seems reasonable in view of the rate constant of exo cyclization of $H_2C{=}CH{-}(CF_2)_3{-}CF_2$ and of $H_2C{=}CH{-}CH_2{-}(CF_2)_3{-}CF_2$ which are, respectively, equal to 11.0 × 10^6 and 19.9 × 10^6 s^{-1}. (b) **7d** is the more reactive radical. Nevertheless, the low value of the $\Delta E^{\ddagger}$ seems in disagreement with the experimental exo rate constant of 14.4 × 10^6 s^{-1},[1d] a value that is only slighty larger than the exo rate constant of **6c**. This point will be discussed again in the following paragraph. In addition, we notice that exo and endo additions occur with nearly the same reaction energy.

2.4. 7-Octenyl Radicals. The contrasting behavior of this radical experimentally observed is well-reproduced by calculations. Indeed, large $\Delta E^{\ddagger}$ values are calculated, and $\Delta E^{\ddagger}$(exo) values are found to be greater than $\Delta E^{\ddagger}$(endo) values in agreement with the low reactivity of this radical and the observed regiochemistry. Moreover, the reaction energy is also affected by this different and striking behavior because, contrary to the former cases, the most stable radical product is the larger ring.

In conclusion, theoretical results have shown their ability to reproduce prominent experimental facts well.

Table 3. Calculated Ionization Potentials, IP (eV), of Some Alkene Fragments

alkene fragment	IP	alkene fragment	IP
$F_2C{=}CF{-}CF_2{-}CF_3$	9.87	$F_2C{=}CF{-}O{-}CF_3$	9.06
$F_2C{=}CH{-}CF_2{-}CF_3$	10.17	$F_2C{=}CH{-}O{-}CF_3$	9.06
$H_2C{=}CH{-}CF_2{-}CF_3$	10.50	$F_2C{=}CH{-}O{-}CH_3$	8.10
$H_2C{=}CH{-}CH_2{-}CF_3$	9.09		

Thus, we are confident in appling theoretical results to obtain information on the determining factors of these intramolecular radical additions.

3. Analysis of the Factors Governing the Reactivity and Regioselectivity in Radical Cyclization. As mentioned in the Introduction, Dolbier et al.[1] essentially attribute the fast rates measured for 5-hexenyl and 6-heptenyl fluorinated radicals to polar effects, which occur when the electrophilic radical and the nucleophilic alkene fragments are brought together. In intermolecular radical addition, polar effects are connected to the participation of the R^-S^+ configuration (R is the electrophilic radical; S is the nucleophilic substrate) to the TS ground-state wave function. The weight of the R^-S^+ configuration to the TS ground state increases concomitantly with the decrease of the alkene ionization potential (IP).[4] Calculated IPs of some alkene fragments are given Table 3.

On the basis of IP values and with the assumption of a predominant contribution of polar effects, we especially expect that **7d** would be more reactive than **7c** and that **5d′** would be more reactive than **5b′** and **5a′**. Indeed, **7d** is found to be more reactive than **7c**, but **5d′** is clearly computed to be less reactive than **5a′** or **5b′**. In addition, natural population analysis (NPA)[20] of starting radicals and of the corresponding TSs does not reveal a real tendency to charge transfer from the alkene moiety to the CF_2 radical fragment. These results seem to indicate that the polar effects do not play such a dominant role in the radical cyclization process. Further studies concerning radical fragments of different polarities are probably necessary to better assess the polar contributions to the reactivity of this kind of reaction and thus give a definitive conclusion.

It has been proposed that entropic contributions provide an explanation for the rate acceleration in intramolecular reactions.[21] To analyze the contribution of nonpotential energy terms, we have calculated kinetic parameters of the cyclization step. They are collected in Table 4.

The $\Delta H^{\ddagger}$ and $\Delta S^{\ddagger}$ values indicated for endo cyclization of **5a** and **5a′** differ from the values calculated by Baker and Dolbier.[7] Our values are relative to the NACs resulting from IRC calculations, whereas Dolbier's values are relative to the open structure. For **5a′**, the energetic profile of the IRC calculations is given in Figure 7.

After ZPE and temperature corrections, the energy barriers are lowered by an almost equal quantity (about 1 kcal mol^{-1}) while reaction energies remain practically unmodified. Changes in entropy are weak for these unimolecular processes; the loss in entropy ranges from −12.1 to −2.1 cal mol^{-1} K^{-1} without any discrimination

(20) Wiberg, K. B.; Rablen, P. R. NPA analysis yields reliable atomic charges. *J. Comput. Chem.* **1993**, *14*, 1504.

(21) (a) Page, M. I.; Jencks, W. P. *Proc. Natl. Acad. Sci. U.S.A.* **1971**, *68*, 1678. (b) Page, M. I.; Jencks, W. P. *Gazz. Chim. Ital.* **1987**, *117*, 455.

Table 4. Kinetic Parameters $\Delta S^{\ddagger}$ (cal mol^{-1} K^{-1}), $\Delta H^{\ddagger}$ (kcal mol^{-1}), and Reaction Enthalpies $\Delta_r H$ (kcal mol^{-1}) for Radical Cyclization Reactions Calculated at 298.15 K[a]

	exo addition			endo addition		
radical	$\Delta H^{\ddagger}$	$\Delta S^{\ddagger}$	$\Delta_r H$	$\Delta H^{\ddagger}$	$\Delta S^{\ddagger}$	$\Delta_r H$
5a	12.3	−5.5	−5.8	12.4	−8.3	−25.2
5a′	6.1	−4.0	−18.5	10.4	−6.2	−29.5
5b	13.2	−6.9	−2.2			
5b′	8.1	−6.8	−11.3			
5c	13.0	−5.6	−6.1			
5c′	7.8	−5.4	−15.4			
5d	13.4	−6.3	−3.0			
5d′	9.6	−5.6	−9.2			
6a	4.1	−6.7	−21.6	4.9	−8.7	−28.4
6a′	1.9	−4.0	−30.8	5.5	−2.1	−31.6
6b	4.3	−7.3	−18.5	6.7	−5.0	−22.7
6c	3.2	−8.0	−18.1	4.1	−8.8	−28.5
7c	1.7	−6.1	−26.3	2.4	−6.3	−26.3
7d	1.1	−10.0	−28.4	2.1	−11.2	−26.2
8d	6.9	−11.0	−20.3	5.8	−12.8	−25.0

[a] Calculated at the B3LYP/6-31G(d) level.

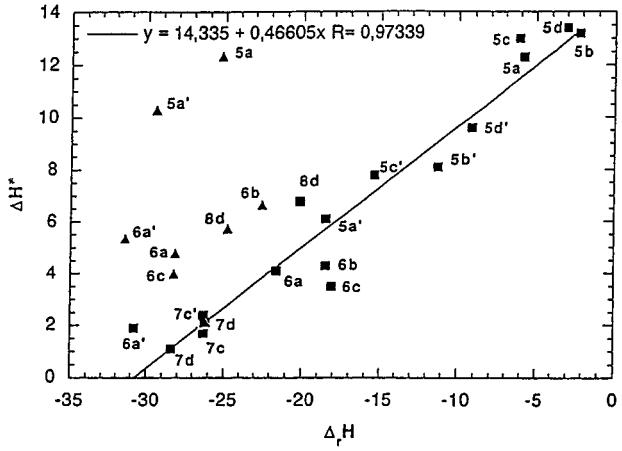

Figure 8. Correlation between activation enthalpy $\Delta H^{\ddagger}$ and reaction enthalpy $\Delta_r H$ for the radical cyclization reactions computed at the UB3LYP/6-31G(d) level: ■, exo cyclization; ▲, endo cyclization.

between exo and endo additions. The larger $\Delta S^{\ddagger}$ values are obtained for the cyclization of **8d** and **7d**. And, it is interesting to note that, for the relative reactivities of **7c** and **7d**, the inclusion of entropic terms leads to a better agreement with experimental data, even if relative reaction barriers well-reproduce general trends of reaction rates.

A good correlation between reaction rates and reaction enthalpies, $\Delta_r H$ (also given in Table 4), is revelant to the strength of the forming bond, usually referred to as the enthalpic effect. We have plotted in Figure 8 activation enthalpies, $\Delta H^{\ddagger}$, against reaction enthalpies, $\Delta_r H$, for the exo and endo cyclizations of fluorinated radicals.

At first sight, Figure 8 exhibits a large scatter of points. However, if we restrain only to data concerning reactions whose TSs are connected to NACs, i.e., **7d** endo addition and all exo additions except **8d**, a good correlation is obtained ($R = 0.973$). Thus, we found that the reaction exothermicity will be a key factor in determining the rate of cyclization of radicals with stable NACs. Then, the assumptions mentioned in the geometrical part (vide supra) found their justification. Moreover, all the systems not considered in the correlation always lie above the correlation line, and the highest deviation corresponds to the endo cyclization of **5a** and **5a′**. Thus, if there is no stable NAC for the starting radical, the cyclization proceeds with a larger $\Delta H^{\ddagger}$ because of the excess of energy needed to get from the conformation of the reactive to that of the TS.

In the case of endo additions of 4-pentenyl and 5-hexenyl radicals, enthalpic effects are opposed to the conformational effects. The antagonism of these two factors is exemplified in **5a**. The thermodynamic contribution greatly favors the endo attack (the endo addition is 20 kcal mol^{-1} more exothermic than the exo one) but is canceled by the work required to bring the radical center of the starting radical above the terminal olefinic carbon center. This work is especially important because of the short length of the radical arm.

The case of the 7-octenyl radical **8d** is different; the absence of stable exo and endo NACs (probably because of the large length of the radical arm) leads to a lesser reactivity of **8d** and to a regiochemistry under thermodynamic control.

6-Heptenyl radicals constitute borderline cases. The cyclization becomes less regioselective because the two determining factors do not efficiently discriminate between the two directions of attack. The exothermicity difference between exo and endo additions is not important, and the conformation of the NAC presents an almost equal distance between the radical center and the two olefinic carbon atoms.

In his study of intramolecular and enzymatic reactions, Bruice pointed out the importance of the mole fraction, *P*, of the NAC on the reaction rates and established a linear correlation between the log of the relative rate constants and log *P*.[17] Our results are in line with the Bruice's conclusion in that, for *P* equals zero, the radical cyclization is a difficult process. *P* is calculated using a Boltzmann distribution and thus necessitates a conformational study of starting radicals. Such a study is out of the scope of this work but remains necessary for a theoretical estimate of relative rate constants of these radical cyclization reactions.

Conclusions

In this paper, we have reported a comprehensive study of radical cyclization reactions. From our results, we can draw the following conclusions:

(1) UB3LYP/6-31G(d) results reproduce the experimental trends very well. Thus, this approach optimizes the often contrasting requests of reliable results and reasonable computational effort. These results suggest also that the B3LYP functional can be confidently used to investigate larger systems in this class of reaction.

(2) Nonpotential energy effects (ZPE, entropy) do not fundamentally alter the trends provided by the only electronic energies.

(3) Two factors seem to play a predominant role in determining the reactivity and the regiochemistry of these intramolecular radical additions. The first factor is the aptitude of the starting radical to exist in a stable conformation for which reaction centers are in position to enter the transition state; our results show that this aptitude is related to the length of the radical arm. As in intermolecular radical additions, the enthalpy of the cyclization reaction, which measures the strength of the forming bond, is the second determining factor. The orientation of the cylization reaction of 4-pentenyl and

5-hexenyl radicals results from a delicate balance between these two factors. Polar effects are not expected to be a determining factor.

Acknowledgment. This work was generously supported by the CNRS. A generous allocation of computer time by the CINES is also gratefully acknowledged.

Supporting Information Available: Optimized geometries and total energies of all compounds and a table similar to Table 1 but listing the geometrical parameters of all the radicals. This material is available free of charge via the Internet at http://pubs.acs.org.

JO0103470